3rd URSI AT-AP-RASC, Gran Canaria, 29 May – 3 June 2022

Far-Field Numerical Radio-Frequency Dosimetry of Insects

Arno Thielens(1)
(1) Department of Information Technology, Ghent University, 9000 Ghent, Belgium, arno.thielens@ugent.be

Abstract

This summary paper provides an overview of our recent work on quantifying far-field radio-frequency electromagnetic field exposure of insects using numerical simulations. To this aim, we have developed a series of 3D digital insect models with associated dielectric parameters. These have been inserted into finite-difference time-domain simulations where they are exposed to incident plane waves from 0.6-240 GHz. This enables one to determine dependencies on frequency and insect type of the RF absorptions in insects.

1. Introduction

Wireless communication is a widespread and growing technology that is enabled by radio-frequency electromagnetic fields (RF-EMFs). Insects are exposed to these fields, which are scattered by their bodies but can also penetrate them [1], [2]. These internal EMFs can have biological effects [3], including dielectric heating [4]. The key to understanding and studying such effects lies in accurate dosimetry, i.e. quantifying EMFs in and around living organisms through measurement or numerical calculation of Maxwell's equations.

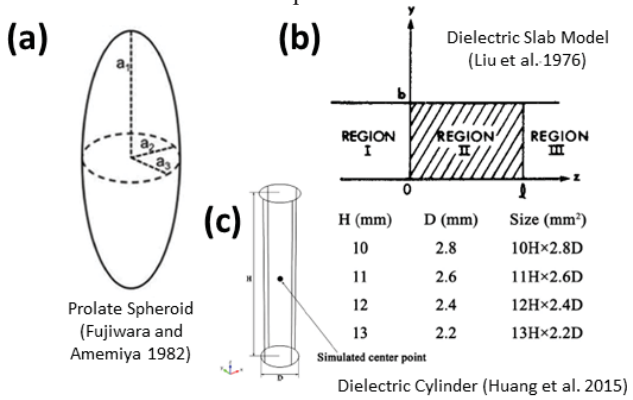

Figure 1. State of the art prior to 2017 in numerical models used in electromagnetic simulations for invertebrates (a) dielectric slab model, (b) spheroidal model, and (c) cylindrical model.

Numerical dosimetry has been very successful for vertebrates [5], [6] for which several highly-detailed models exist [7], [8]. In contrast, studies that focus on numerical dosimetry of insects are nearly non-existent. Up to very recently (prior to 2017), the state-of-the-art in this field consisted out of studies that modelled invertebrates as simplified geometric shapes (spheroids, cylinders) or using one-dimensional approximations such as a dielectric slab [9]–[11], see Figure 1. Hence, there is little known on how EMFs are distributed in and around invertebrates [10].

In order to partially close this knowledge gap, our recent work has been focused on quantifying far-field exposure of insects. We study far-field exposure, because our measurements have shown that far-field exposure is the dominant source of insect exposure in [2] and have been able to show that absorption of RF-EMFs in insects depend on the frequency of exposure. However, up to now it is unclear how this frequency-dependency varies from one insect species to another. This publication tries to answer this question, by synthesizing our prior results.

2. Materials and Methods

Subsection 2.1 outlines the methods we used to develop insect models and their dielectric properties. These models and dielectric properties can be combined into numerical simulations where far-field RF-EMF exposure can be modeled, as described in Subsection 2.2.

2.1 Insect Model Development

A series of insects in different developmental stages have been scanned using micro-computerized tomography (CT) scanners [12]. Scanning of the insects resulted in a stack of images for each specimen. These images were analyzed in order to identify those pixels that are part of the insect in each slice. The slices are then combined in specialized imaging processing software in order to obtain 3D models. The spatial resolution of the models is preferential of the order of tens to hundreds of μm, because this leads to a more accurate representation of the insect and avoids losing interconnects in the model, which can lead to losses of currents within the model. This is illustrated in Fig. 2. Additionally, some numerical techniques require a frequency-dependent minimal spatial resolution in the simulation domain.

The distribution of EMFs inside and around the 3D insect models depends on their dielectric parameters, i.e. the relative permittivity (ε_r) and conductivity (σ). In order to estimate these parameters for insects, we have executed

and a literature review of previous studies that measured of dielectric properties of insects in the RF range [13]–[16]. Additionally, we have also performed our own measurements of dielectric properties of the Yellow Fever Mosquito (*Aedes aegypti*) with a dielectric assessment kit for thin layers, using a methodology described in [17].

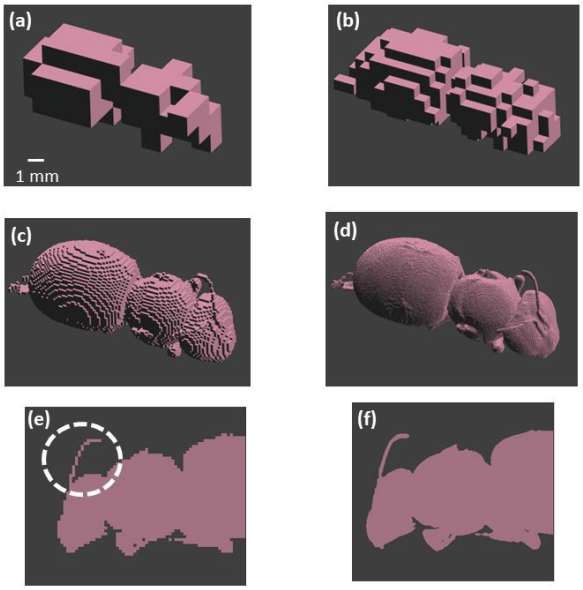

Figure 2. 3D model of a Western Honey Bee Worker (*Apis mellifera*), voxelled with (a) 1 mm, (b) 0.5 mm, (c) 100 μm, and (d) 20 μm resolution. Transverse slices of the same model with (e) 100 μm, and (f) 20 μm resolution, demonstrating loss of interconnection in the bee's antennae (indicated by the white, dashed circle).

2.2 Numerical Simulations of Far-Field RF-EMF Exposure of Insects

The insect models are used in finite-difference time-domain (FDTD) simulations in the commercial software Sim4life (ZMT, Zürich, Switzerland). In the far-field regime, the RF source (antenna) and the exposed insect are decoupled, which allows one to model the exposure as a set of plane waves [18]. In these insect simulations, far-field exposure is modelled as plane waves incident from the top and bottom of the insect's main longitudinal axis, and two directions on two orthogonal axes in the mid-transverse plane orthogonal to this axis. In each direction we simulated 2 orthogonal polarizations, leading to twelve simulations per frequency per insect. This approach of using a set of omnidirectional plane waves has been used previously for humans [18], [19] to model far-field exposure with unknown angle of incidence.

All insects were simulated at 2, 3, 6, 12, 24, 60, and 120 GHz. The honey bees, see Table I, were also simulated at 0.6 and 1.2 GHz, while the mosquitoes, see Table I, were also simulated at 90, 180, and 240 GHz. We used dielectric properties from literature (see Table II) for all studied insects, except for the mosquitoes for which we used our own measurements. More information on the precise simulation settings can be found in [1], [2], [17]. All these simulations lead to a distribution of internal electric fields ($\bar{E}_{int}$) within the studied insect. From these electric fields, the absorbed power (P_{abs}) can be determined using:

$$P_{abs} = \int_V \sigma . |\bar{E}_{int}|^2 dV \quad (1).$$

with V the volume of the insect and σ its conductivity. The P_{abs} is then averaged over all 12 plane waves.

3. Results and Discussion

3.1 Insect Models

Table I. Insect models with resolution and volume

Insect Name	Lossy Volume (mm^3)	Resolution (μm)	Ref.
Australian Stingless Bee	6.2	5	[1]
Beetle	21	10	[1]
Desert locust	1859	10	[1]
Honey Bee Worker 1	55	20	[1]
Honey Bee Worker 2	162	100	[2]
Honey Bee Drone	368	100	[2]
Honey Bee Queen	310	250	[2]
Honey Bee Larva	512	20	[2]
Female Y-F Mosquito (3)	1.1-1.4	4	[17]
Male Y-F Mosquito (3)	0.7-0.9	4	[17]

Table II. Dielectric properties of insects (taken from [1])

Frequency (GHz)	$\varepsilon_r(.)$	$\sigma\,(\frac{S}{m})$
2	39.9	1.35
3	38.8	2.05
6	38	5.05
12	26	11.5
24	14.9	21.1
60	7.02	27.9
120	5.46	29.2

Up to now, we developed 14 insect models of the following species: one Australian Stingless Bee (*Tetragonula carbonaria*), five models of Western Honey bees (*Apis mellifera*) in different developmental stages, one Desert Locust (*Schistocerca gregaria*), one Beetle (*Geotrupes stercorarius*), and six models of Yellow Fever Mosquito (*Aedes aegypti*). The volumes and spatial resolutions of these models are listed in Table I and Figure 3 (a) shows an example of one of the models developed for a Honey Bee Worker (nr. 1). Given the relatively broad range in these insects' volumes, 0.7-1859 mm^3, one can expect a large variation in absorbed power at a given frequency and strong differences in frequency dependency. Our literature review showed that most studies investigate insect dielectric properties using the coaxial-line probe method [13]–[16]. We found similar trends as function of frequency for different insects and averaged dielectric

parameter values found in literature to obtain those shown in Table II [1].

3.2 Far-Field RF-EMF absorption in Insects

Numerical simulation using an insect model will commonly result in a distribution of EMFs fields inside and around the insect. Fig. 3 (b) shows an example of such a field distribution inside and around a honey bee worker at 12 GHz under single plane wave exposure. The P_{abs} can be determined from these fields using Eq. 1.

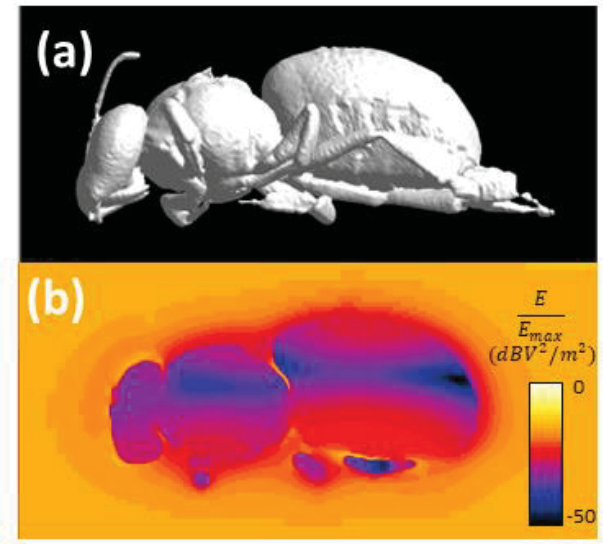

Figure 3. (a)Micro-CT-model of a Honey Bee Worker, and (b) Relative E-field distribution at 12 GHz around the same model for a plane wave incident from below.

When considering far-field exposure, all of the studied insects show a similar trend in average P_{abs} as function of frequency. There is a strong increase in P_{abs} from sub-GHz frequencies up to a maximum located at 6 GHz or higher, after that there is a stabilization or a slight decrease in P_{abs} [1], [2], [17]. Fig. 4 shows an example of P_{abs} as function of frequency for one of the studied honey bee workers.

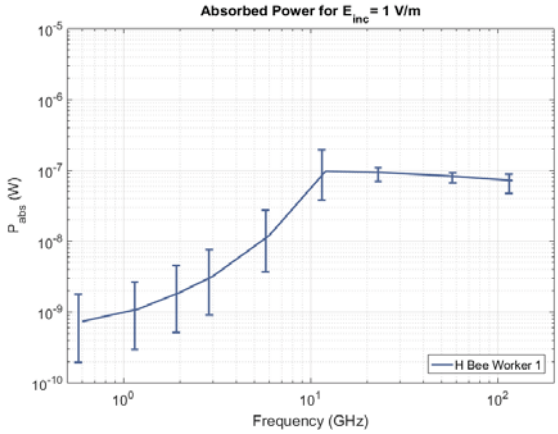

Figure 4. P_{abs} in the Honey Bee worker 1 as function of frequency, normalized to an incident plane-wave field strength of 1 V/m at each frequency. The curves indicate the mean values over the twelve plane wave simulations, while the whiskers indicate the maximum and minimum values found at each frequency.

Our simulations show that the mean absorbed RF power within an insect increases from 0.6 – 6 GHz for a constant incident power density for all of the studied insects. The two largest studied insects, i.e. the honey bee larva and desert locust, have their peak absorption at 6 GHz, while the other insects have their peak absorption at higher frequencies. Fig. 5 shows the simulated frequency where we found the maximal average far-field P_{abs} as function of the insect volume. We found that in general the frequency of maximal absorption decreases with insect volume. These results are in line with what was found for vertebrates in [20] and what was found for the smaller subsets studied in [1], [2], [17].

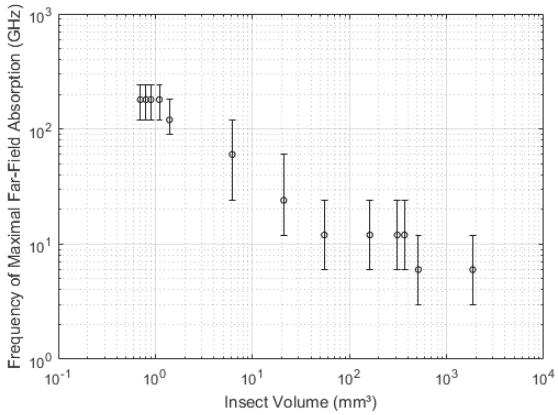

Figure 5. Frequency of maximal RF-EMF absorption in insects as function of insect volume. The markers indicate the simulated frequency where max P_{abs} was found, while the whiskers show the resolution in simulated frequencies.

When considering a constant incident field strength, the maximal, average P_{abs} found for a particular insect increases with volume. The maximal average absorbed power for an incident field strength of 1 V/m found in any of the studied insects was 1.2 μW for the Desert Locust at 6 GHz. On the other hand of the spectrum, we found a maximal aveage P_{abs} for the smallest male mosquito of 30 nW for the same incident field strength, at 180 GHz. A similar decrease of maximal, average P_{abs} with volume was found for humans at lower RF frequencies [18]–[20].

4. Conclusions and Future Research

We have developed 14 insect models with associated dielectric properties. These have been used in FDTD simulations of plane wave exposure at frequencies from 0.6-240 GHz to study far-field RF-EMF exposure. These simulations have demonstrated that for all studied insects the far-field absorbed power increases up to 6 GHz. Insects have a frequency of maximal absorption that depends on their volume. The maximal average absorbed power for an incident field strength of 1 V/m found in any of the studied insects was 1.2 μW. In our future research, we will develop heterogeneous insect models, which should be more accurate representations of reality than the currently used homogeneous models. We will also extend our work to modelling exposure near (realistic) antennas, for which the first steps have been taken in [21].

6. Acknowledgements

A.T. is a postdoctoral fellow of the Research Foundation Flanders (FWO) under grant agreement no. 1283921N. This work was partly funded by the FWO under grant agreement no. G033220N. A.T thanks his collaborators on this research topic.

References

[1] A. Thielens, D. Bell, D. B. Mortimore, M. K. Greco, L. Martens, and W. Joseph, "Exposure of Insects to Radio-Frequency Electromagnetic Fields from 2 to 120 GHz," *Sci Rep*, vol. 8, no. 1, p. 3924, Dec. 2018, doi: 10.1038/s41598-018-22271-3.

[2] A. Thielens, M. K. Greco, L. Verloock, L. Martens, and W. Joseph, "Radio-Frequency Electromagnetic Field Exposure of Western Honey Bees," *Sci Rep*, vol. 10, no. 1, p. 461, Dec. 2020, doi: 10.1038/s41598-019-56948-0.

[3] S. Cucurachi, W. L. M. Tamis, M. G. Vijver, W. J. G. M. Peijnenburg, J. F. B. Bolte, and G. R. de Snoo, "A review of the ecological effects of radiofrequency electromagnetic fields (RF-EMF).," *Environment international*, 2013, doi: 10.1016/j.envint.2012.10.009.

[4] Nelson, "Review and Assessment of Radio-frequency and Microwave Energy for Stored-grain Insect Control," *Transactions of the ASAE*, vol. 39, no. 4, pp. 1475–1484, 1996, doi: 10.13031/2013.27641.

[5] C.-K. Chou, "A need to provide explanations for observed biological effects of radiofrequency exposure," *Electromagnetic Biology and Medicine*, vol. 34, no. 3, pp. 175–179, Jul. 2015, doi: 10.3109/15368378.2015.1076439.

[6] C.-K. Chou *et al.*, "Radio frequency electromagnetic exposure: Tutorial review on experimental dosimetry," *Bioelectromagnetics*, p. 14, 1996.

[7] M.-C. Gosselin *et al.*, "Development of a new generation of high-resolution anatomical models for medical device evaluation: the Virtual Population 3.0," *Phys. Med. Biol.*, vol. 59, no. 18, pp. 5287–5303, Aug. 2014, doi: 10.1088/0031-9155/59/18/5287.

[8] Y. Gong *et al.*, "Life-Time Dosimetric Assessment for Mice and Rats Exposed in Reverberation Chambers of the 2-Year NTP Cancer Bioassay Study on Cell Phone Radiation," p. 37, 2018.

[9] Z. Huang, L. Chen, and S. Wang, "Computer simulation of radio frequency selective heating of insects in soybeans," *International Journal of Heat and Mass Transfer*, vol. 90, pp. 406–417, Nov. 2015, doi: 10.1016/j.ijheatmasstransfer.2015.06.071.

[10] O. Fujiwara and Y. Amemiya, "Microwave Power Absorption in a Biological Specimen Inside a Standing-Wave Irradiation Waveguide," *IEEE Trans. Microwave Theory Techn.*, vol. 30, no. 11, pp. 2008–2012, Nov. 1982, doi: 10.1109/TMTT.1982.1131360.

[11] L. M. Liu, F. J. Rosenbaum, and W. F. Pickard, "Electric-Field Distribution Along Finite Length Lossy Dielectric Slabs in Waveguide," *IEEE Trans. Microwave Theory Techn.*, vol. 24, no. 4, pp. 216–219, Apr. 1976, doi: 10.1109/TMTT.1976.1128819.

[12] T. Bultreys *et al.*, "Fast laboratory-based micro-computed tomography for pore-scale research: Illustrative experiments and perspectives on the future," *Advances in Water Resources*, vol. 95, pp. 341–351, Sep. 2016, doi: 10.1016/j.advwatres.2015.05.012.

[13] S. Wang, J. Tang, R. P. Cavalieri, and D. C. Davis, "Differential Heating of Insects in Dried Nuts and Fruits Associated with Radio Frequency and Microwave Treatments," *Transactions of the ASAE*, vol. 46, no. 4, 2003, doi: 10.13031/2013.13941.

[14] Nelson, P. G. Bartley, Jr., and K. C. Lawrence, "RF and Microwave Dielectric Properties of Stored-Grain Insects and Their Implications for Potential Insect Control," *Transactions of the ASAE*, vol. 41, no. 3, pp. 685–692, 1998, doi: 10.13031/2013.17194.

[15] J. Ondráček and V. Brunnhofer, "Dielectric properties of insect tissues. - Abstract - Europe PMC," *Gen. Physiol. Biophys*, 1984, Accessed: Aug. 21, 2020. [Online]. Available: https://europepmc.org/article/med/6479581

[16] B. Colpitts, Y. Pelletier, and S. Cogswell, "Complex Permittivity Measurements of the Colorado Potato Beetle Using Coaxial Probe Techniques," *Journal of Microwave Power and Electromagnetic Energy*, vol. 27, no. 3, pp. 175–182, Jan. 1992, doi: 10.1080/08327823.1992.11688187.

[17] E. De Borre *et al.*, "Radio-frequency exposure of the yellow fever mosquito (A. aegypti) from 2 to 240 GHz," *PLOS Computational Biology*, vol. 17, no. 10, p. e1009460, Oct. 2021, doi: 10.1371/journal.pcbi.1009460.

[18] I. Liorni *et al.*, "Evaluation of Specific Absorption Rate in the Far-Field, Near-To-Far Field and Near-Field Regions for Integrative Radiofrequency Exposure Assessment," *Radiation Protection Dosimetry*, vol. 190, no. 4, pp. 459–472, Oct. 2020, doi: 10.1093/rpd/ncaa127.

[19] J. F. Bakker, M. M. Paulides, A. Christ, N. Kuster, and G. C. van Rhoon, "Assessment of induced SAR in children exposed to electromagnetic plane waves between 10 MHz and 5.6 GHz," *Phys. Med. Biol.*, vol. 56, no. 9, pp. 2883–2883, May 2011, doi: 10.1088/0031-9155/56/9/2883.

[20] C. Durney, H. Massoudi, and M. Iskander, *Radiofrequency Radiation Dosimetry Handbook*. 1986.Available:http://niremf.ifac.cnr.it/docs/HANDBOOK/home.htm

[21] D. Toribio, W. Joseph, and A. Thielens, "Near Field Radio-Frequency Electromagnetic Field Exposure of a Western Honey Bee," *IEEE Transactions on Antennas and Propagation*, pp. 1–1, 2021, doi: 10.1109/TAP.2021.3111286.